



Cite this: *Phys. Chem. Chem. Phys.*,
2017, **19**, 10292

Change of the isoelectric point of hemoglobin at the air/water interface probed by the orientational flip-flop of water molecules†

Stéphanie Devineau,[‡] Ken-ichi Inoue,^a Ryoji Kusaka,^{§a} Shu-hei Urashima,^a Satoshi Nihonyanagi,[‡] Damien Baigl,^{bc} Antonio Tsuneshige^e and Tahei Tahara^{*ad}

Elucidation of the molecular mechanisms of protein adsorption is of essential importance for further development of biotechnology. Here, we use interface-selective nonlinear vibrational spectroscopy to investigate protein charge at the air/water interface by probing the orientation of interfacial water molecules. We measured the $\text{Im}\chi^{(2)}$ spectra of hemoglobin, myoglobin, serum albumin and lysozyme at the air/water interface in the CH and OH stretching regions using heterodyne-detected vibrational sum frequency generation (HD-VSFG) spectroscopy, and we deduced the isoelectric point of the protein by monitoring the orientational flip-flop of water molecules at the interface. Strikingly, our measurements indicate that the isoelectric point of hemoglobin is significantly lowered (by about one pH unit) at the air/water interface compared to that in the bulk. This can be predominantly attributed to the modifications of the protein structure at the air/water interface. Our results also suggest that a similar mechanism accounts for the modification of myoglobin charge at the air/water interface. This effect has not been reported for other model proteins at interfaces probed by conventional VSFG techniques, and it emphasizes the importance of the structural modifications of proteins at the interface, which can drastically affect their charge profiles in a protein-specific manner. The direct experimental approach using HD-VSFG can unveil the changes of the isoelectric point of adsorbed proteins at various interfaces, which is of major relevance to many biological applications and sheds new light on the effect of interfaces on protein charge.

Received 28th December 2016,
Accepted 15th March 2017

DOI: 10.1039/c6cp08854f

rsc.li/pccp

Introduction

Protein adsorption at interfaces is a ubiquitous feature in biotechnology. Indeed, protein immobilization on surfaces is usually required in biocatalysis^{1,2} and for immunoassays.³ Foam formation and stability in food products also requires the effective control of protein adsorption at the air/water interface.^{4–6} However, protein adsorption turns out to be an unwanted effect

when it results in the fouling of food processing reactors, biosensors,⁷ and biomedical devices⁸ potentially leading to adverse immune reactions to biomaterials.⁹ The adsorption of therapeutic proteins at the air/water interface during the production process also poses a potential risk to patients if it leads to structural modifications in the final product.¹⁰ Understanding the mechanisms of protein adsorption has been a long standing topic that nonetheless still requires much attention to improve the design of anti-fouling surfaces,¹¹ to reduce bacterial adhesion¹² and to develop new lab-on-chip device for protein purification and medical diagnosis.¹³ The relevant molecular mechanisms occurring at interfaces have not been fully unraveled, preventing proper control and prediction of protein adsorption.

Protein conformation at the interface has been studied using a wide range of techniques, such as infrared,^{14,15} fluorescence,^{16,17} and nonlinear spectroscopy,¹⁸ circular dichroism,¹⁹ ellipsometry,²⁰ and X-ray²¹ and neutron reflectivity.²² The dynamics of adsorbed proteins was recently investigated by fluorescence,²³ NMR²⁴ and neutron scattering.²⁵ Thermodynamics studies²⁵ and MD simulations²⁶ pointed out the key role of water displacement and restructuring in protein adsorption, suggesting that an

^a Molecular Spectroscopy Laboratory, RIKEN, 2-1 Hirosawa, Wako, Saitama 351-0198, Japan. E-mail: tahei@riken.jp

^b Ecole Normale Supérieure, PSL Research University, UPMC Univ Paris 06, CNRS, PASTEUR, Department of Chemistry, 24 rue Lhomond, 75005 Paris, France

^c Sorbonne Universités, UPMC Univ Paris 06, ENS, CNRS, PASTEUR, 75005 Paris, France

^d Ultrafast Spectroscopy Research Team, RIKEN Center for Advanced Photonics Centre (RAP), RIKEN, 2-1 Hirosawa, Wako, Saitama 351-0198, Japan

^e Faculty of Bioscience and Applied Chemistry, Hosei University, Tokyo, Japan

† Electronic supplementary information (ESI) available. See DOI: 10.1039/c6cp08854f
‡ Present address: Centre for BioNano Interactions, University College Dublin, Belfield, Dublin 4, Ireland.

§ Present address: Nuclear Science and Engineering Center, Japan Atomic Energy Agency (JAEA), 2-4 Shirakata, Tokai-mura, Ibaraki 319-1195, Japan.

additional hydration layer may prevent protein adhesion.^{8,27} However, most of the techniques that probe protein structure do not capture changes of water molecule organization at the interface. It is thus important to investigate both protein and interfacial water structures at the molecular scale to better understand the adsorption process.²⁸ Moreover, interfaces have peculiar physicochemical properties which are different from the bulk such as a more acidic pH at the air/water interface^{29–31} and a different polarity sensed by adsorbed molecules.³² It is not clear whether proteins would retain the same charge at the interface compared to the bulk, and only a few experimental studies have investigated this point.^{5,33,34}

Vibrational sum frequency generation (VSFG) spectroscopy is a powerful and versatile interface-specific technique to study molecules at various interfaces.^{35–38} The second-order nonlinear susceptibility $\chi^{(2)}$ is nonzero only in the region where the inversion symmetry is broken, such as interfaces. Thus, VSFG selectively measures the vibrational spectra of oriented molecules at the interface without any contribution from the bulk under the dipole approximation. In particular, VSFG spectroscopy provides rich information about water structure at the interface by measuring the OH stretching band whose frequency directly reflects the hydrogen (H-) bond strength of water molecules.³⁷

VSFG has been applied to protein adsorption at the air/water interface.^{5,33,36,39–41} Protein adsorption leads to surface charging and it is expected that charge–dipole interaction induces orientation of water molecules at the interface.⁴² In fact, in the VSFG studies of lysozyme³⁹ and BSA^{5,36} adsorption, the intensity change of the OH stretching band was observed with the change of pH, which suggests that the change of the protein charge induces a change of water molecule orientation at the interface. In the case of lysozyme and BSA, the point of zero net charge appeared to be similar in the bulk and at the air/water interface. However, in conventional homodyne-detected VSFG, the signal measured is proportional to $|\chi^{(2)}|^2$ and loses information on the $\chi^{(2)}$ phase, which prevents direct observation of the OH orientation that is sensitive to the protein charge. Furthermore, the contribution of each vibrational mode can be positive or negative, and its interference distorts the vibrational spectrum obtained by $|\chi^{(2)}|^2$ measurements. This often misleads the spectrum analysis. It is thus highly desirable to examine and discuss protein adsorption not on the $|\chi^{(2)}|^2$ spectra but on the $\chi^{(2)}$ spectra themselves.

The recent development of heterodyne-detected VSFG spectroscopy (HD-VSFG) can bring new insights in this topic by directly probing the water molecule orientation at the interface together with protein adsorption. HD-VSFG gives access to the real (Re) and the imaginary (Im) parts of $\chi^{(2)}$.^{42–47} The spectral shape in Im $\chi^{(2)}$ spectra can be interpreted in the same manner as IR absorption or Raman spectra of molecules in the bulk.³⁵ Moreover, the sign of Im $\chi^{(2)}$ in the OH stretching region directly indicates the up or down average orientation of water molecules while that in the CH stretching region provides information on the orientation of the methyl groups and the aromatic rings of the adsorbed proteins. HD-VSFG spectroscopy has been applied to aqueous interfaces and revealed various new insights.^{42,43,48–50}

Very recently, it has also been used to study protein/water interfaces with the antifreeze protein DAFP-1⁵¹ and α -lactalbumin.⁵²

In this paper, we report an HD-VSFG study of water structure and orientation at various air/protein/water interfaces. Hemoglobin (HbA), serum albumin (BSA), myoglobin (Mb) and lysozyme (Lz) were chosen as model globular proteins exhibiting a large range of isoelectric points in the bulk: ~ 4.8 for BSA,⁵³ 7.0 for HbA,⁵⁴ 7.4 for Mb,^{55,56} and 11.3 for Lz.⁵⁷ We show that HD-VSFG is sensitive enough to detect the decrease by one pH unit of the isoelectric point of human hemoglobin at the air/water interface.

Experimental

Proteins

Human adult hemoglobin was obtained from fresh blood drawn into tubes containing ethyldiaminetetraacetate by venipuncture of the median cubital vein of a healthy, non-smoker adult, at the clinic of the Hosei University, Koganei Campus, in accordance with the local, academic and legal procedures and guidelines. HbA was purified following standard procedures,⁵⁸ with some modifications as described in the ESI.† HbA in the oxygenated form was aliquoted and stored at -80 °C. HbA integrity was checked by measuring the absorption ratios at 576 nm and 541 nm, which are indicative of iron oxidation and protein damage.⁵⁹ Lyophilized horse-heart metmyoglobin (Sigma, M1882) and bovine serum albumin (Sigma, A0281) were dissolved and dialyzed in pure water. Lysozyme from chicken egg white (Sigma, L7651) was dissolved in phosphate buffer at pH 7.4. All the protein solutions were centrifuged at 14 000g for 5 min at 4 °C before use. Protein concentrations were determined by UV-vis spectroscopy on a Hitachi U-3310 spectrophotometer.^{55,60} HbA concentration is expressed as heme molar concentration.

Chemicals

D₂O (NMR grade, 99.9%) was purchased from Wako. Phosphate buffers from pH 5.0 to pH 9.0 were prepared by dissolving monosodium and disodium phosphate (Wako) in pure MilliQ-water (MilliPore, 18.2 M Ω cm resistivity). All the experiments were performed in 50 mM phosphate buffer.

HD-VSFG

The experimental set-up of multiplex HD-VSFG used in this study was described previously.⁴⁹ Briefly, the light source of the setup was a Ti:sapphire regenerative amplifier (Spectra Physics, Spitfire Ace, average power ~ 5.0 W, repetition rate 1 kHz, pulse width ~ 80 fs). A part of the amplifier output passed through a narrow band-pass filter (CVI Melles Griot, center wavelength 795 nm, bandwidth 1.5 nm) to produce a narrowband visible pulse (ω_1). The other part of the output pumped a commercial optical parametric amplifier (Spectra Physics, TOPAS Prime) to generate broadband IR pulses (ω_2 , center wavelength 2750, 3000 and 3400 nm, bandwidth ~ 300 cm⁻¹). The ω_1 and ω_2 pulses were focused on and transmitted through an ultrathin y -cut quartz crystal (10 μ m thickness). When the ω_1 and ω_2 pulses were spatially and temporally overlapped, the sum frequency (SF1)

was generated at $\omega_3 = \omega_1 + \omega_2$. The ω_1 and ω_2 pulses and SF1 were refocused at the surface of the solution with a spherical concave mirror to generate the sum frequency of the sample (SF2). SF1 was delayed by ~ 3.3 ps with respect to SF2 by passing through a 2 mm thick silica plate. SF1 and SF2 pulses were introduced into a polychromator where they were dispersed and temporally stretched to produce interference fringes in the frequency domain. The interference fringes were detected by a charge-coupled device (CCD) (Princeton Instruments, Spec-10:2KB). The frequency domain spectrum was inverse Fourier transformed and the heterodyne signal was extracted by using a filter function in the time domain. The heterodyne signal was then Fourier transformed back to the frequency domain. An equivalent heterodyne signal from a z-cut quartz was recorded as the reference for calibrating the intensity and the phase of the sample spectrum. Using this procedure, the corrected imaginary (Im) and real (Re) $\chi^{(2)}$ spectra of the sample were obtained. Three complex $\chi^{(2)}$ spectra were measured with different ω_2 , and they were combined to fully cover the CH and OH stretching regions. Sum frequency, visible and IR pulses were *s*, *s* and *p* polarized, respectively (*ssp* configuration). The height of the solution surface was monitored by a displacement sensor (Keyence, SI-F10) and maintained constant with an accuracy of 1 μm during the measurements. The phase accuracy was checked by measuring the Im $\chi^{(2)}$ spectrum of the air/D₂O interface (Fig. S1, ESI[†]). The Im $\chi^{(2)}$ is zero within the signal to noise ratio in the OH stretching region. Protein solutions were equilibrated for 20 min in a glass cell at 296 K before starting the measurements. Each $\chi^{(2)}$ spectrum is the average of at least three independent measurements.

Results

Adsorption of hemoglobin (HbA) at the air/water interface

First, we studied the adsorption of HbA at the air/water interface by measuring the Im $\chi^{(2)}$ spectra in the CH and OH stretching regions. HbA is a tetrameric protein composed of two α -chains and two β -chains. Its isoelectric point in bulk water is 7.0.⁵⁴ Before protein adsorption, the Im $\chi^{(2)}$ spectrum of water at the air/neat water interface exhibits two characteristic OH stretching bands at ~ 3450 cm^{-1} and ~ 3700 cm^{-1} (Fig. 1, black line). The negative low frequency band is assigned to the H-bonded OH with H-down orientation (towards bulk water) and the positive high frequency band corresponds to free OH, which is OH with no H-bond, with H-up orientation (towards the air).^{35,43,61} By adding HbA to phosphate buffer at pH 7.4, drastic changes are observed in the aliphatic CH (2800–3000 cm^{-1}), aromatic CH (~ 3060 cm^{-1}), H-bonded OH (3000–3600 cm^{-1}) and the free OH (3700 cm^{-1}) regions, as shown in Fig. 1. The CH bands appear, the H-bonded OH band changes its shape and sign, and free OH decreases. The disappearance of the free OH band for [HbA] ≥ 1 μM suggests that the surface is fully covered with adsorbed HbA under this condition. Furthermore, no temporal evolution of the Im $\chi^{(2)}$ spectra in the CH and OH stretching regions was observed, confirming that protein damage under laser irradiation is negligible under the present experimental conditions (Fig. S2, ESI[†]).

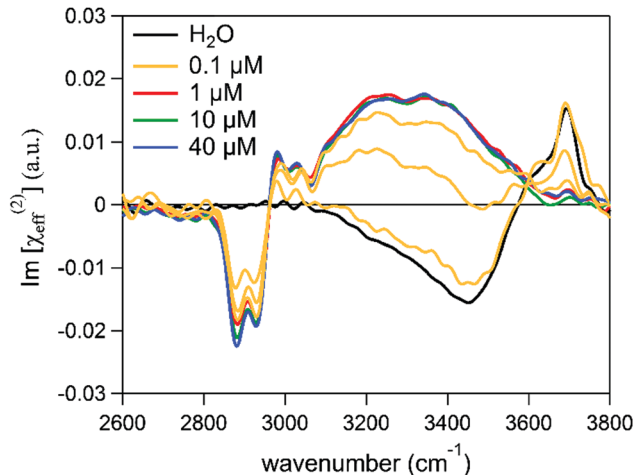


Fig. 1 Imaginary $\chi^{(2)}$ spectra in the CH and OH stretching regions of HbA at a concentration of 0.1, 1, 10 and 40 μM in 50 mM phosphate buffer at pH 7.4. The spectrum of the air/neat water interface is also shown for comparison.

The negative bands at ~ 2880 cm^{-1} and ~ 2930 cm^{-1} are assigned to the symmetric CH stretching vibrations of methyl groups split by the Fermi resonance with the bending overtone.^{36,39} The positive band at ~ 2980 cm^{-1} corresponds to the anti-symmetric CH stretching of methyl groups. Because Im $\chi^{(2)}$ originates only from interfacial molecules, this confirms spontaneous adsorption of HbA at the air/water interface from the solution. Aliphatic amino acids containing one (Ala, Met, Thr) or two (Leu, Ile, Val) CH_3 groups are present in both α -chain and β -chain subunits of a HbA tetramer, and the total number of methyl groups per protein is 380 (Fig. 2a). The observed negative sign of the methyl symmetric CH stretching indicates an average H-up orientation of methyl groups that are pointing towards the air.^{42,62} The CH stretching of methylene groups

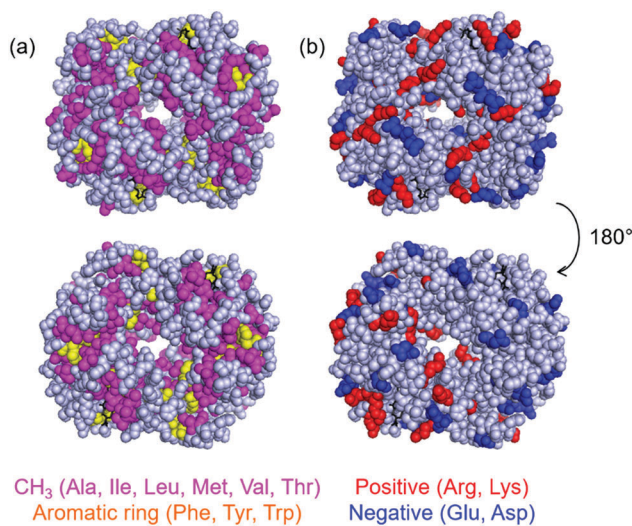


Fig. 2 Localization of (a) residues having CH_3 groups or an aromatic ring, and (b) positively charged or negatively charged residues in tetrameric HbA in the bulk (structure PDB 1B86).

which could be expected at $\sim 2920\text{ cm}^{-1}$ is not prominent in the present $\text{Im } \chi^{(2)}$ spectra.⁶³ The low intensity negative band at $\sim 3060\text{ cm}^{-1}$, which is lifted by both the methyl antisymmetric CH stretching band at $\sim 2980\text{ cm}^{-1}$ and the broad OH band of water peaked around $\sim 3300\text{ cm}^{-1}$, is assignable to the aromatic CH stretching³⁶ of HbA. By comparison with the IR and Raman spectra, the two most probable vibrational modes of phenyl CH stretching at this frequency are ν_2 at 3055 cm^{-1} and ν_{20} at 3063 cm^{-1} .^{64,65} Both vibrational modes have negative hyperpolarizability,⁶⁴ indicating that aromatic rings are oriented towards the air similarly to the CH_3 groups. HbA contains 36 aromatic residues (Phe, Tyr, Trp) distributed in both subunits (Fig. 2a and Table S1, ESI[†]).

The large broad band arising at $\sim 3300\text{ cm}^{-1}$ is assigned to the OH stretching of water molecules near the protein which is adsorbed at the air/water interface. The contribution to the OH stretching of Ser, Thr and Tyr residues is considered negligible due to the large number of surrounding water molecules compared to these residues. The OH band shifts towards a lower frequency compared to neat water, indicating a stronger H-bonding of the water network at the protein surface. Moreover, the sign of the H-bonded OH band becomes positive when HbA is adsorbed at the air/water interface, implying that orientation of water molecules changes from H-down to H-up. The H-up orientation for the HbA-adsorbed interface at pH 7.4 is the key finding of the present study and we will further discuss this result in the next section.

We note that the $\text{Im } \chi^{(2)}$ spectrum measured for $[\text{HbA}] = 0.1\text{ }\mu\text{M}$ varied significantly for each experiment (Fig. S3a, ESI[†]). Given the limited area probed by the laser spot (beam diameter $\sim 100\text{ }\mu\text{m}$), this could possibly be due to partial protein coverage: the amount of HbA would not be sufficient to entirely cover the water surface. In fact, although the $\text{Im } \chi^{(2)}$ spectrum measured for $[\text{HbA}] = 0.1\text{ }\mu\text{M}$ varied largely, all the spectra are intermediate between the spectra of $10\text{ }\mu\text{M}$ HbA solution and neat water and, more importantly, they are well fitted by a linear combination of the two spectra (Fig. S3b and Table S2, ESI[†]). This strongly suggests that the variation of the spectra measured at $[\text{HbA}] = 0.1\text{ }\mu\text{M}$ is due to inhomogeneity of the protein adsorption and resultant different protein coverage in the small laser spot moment to moment. It is known that the conformation of adsorbed proteins on solid surfaces^{66–68} and at the air/water interface^{40,69} depends on surface coverage: a lower surface coverage can lead to higher structural modifications. However, the present result shows that even the spectrum of interfacial water at the low coverage is well reproduced by a linear combination of the spectra of full and no coverage, indicating that the water structure close to HbA does not change with protein surface coverage. In particular, the spectra are essentially the same for all HbA concentrations above $1\text{ }\mu\text{M}$.

$\text{Im } \chi^{(2)}$ spectra of HbA solution at the air/water interface as a function of pH

The spectral shape of the H-bonded OH in the $\text{Im } \chi^{(2)}$ spectra changes drastically with pH when HbA is adsorbed at the interface, as shown in Fig. 3. At pH 5, the OH stretching band is

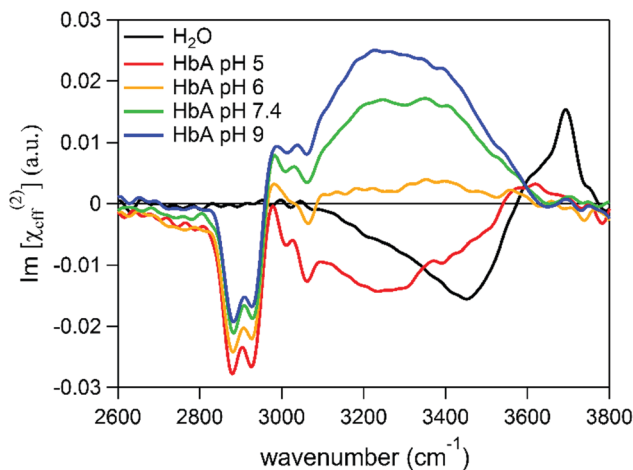


Fig. 3 Imaginary $\chi^{(2)}$ spectra in the CH and OH stretching regions of $10\text{ }\mu\text{M}$ HbA in 50 mM phosphate buffer at bulk pH 5, 6, 7.4 and 9 at the air/water interface.

negative for HbA solution, indicating H-down orientation of water molecules at the interface. The intensity of the OH stretching bands of HbA solution at pH 5 and neat water are comparable, indicating a similar degree of net orientation at the interface. The OH stretching band intensity for HbA solution gets weaker as pH increases and becomes minimum around pH 6. Then, the positive OH stretching band appears and the intensity increases from pH 6 to pH 9. Because no change of water orientation is observed for buffer solutions without HbA (Fig. S1, ESI[†]), it is safe to conclude that the observed orientational flip-flop of water molecules is induced by the adsorption of HbA at the air/water interface. (Note that HbA in bulk solution is stable in this pH range.⁵⁵) The small positive band visible at $\sim 3600\text{ cm}^{-1}$ at pH 5 can be assigned to the OH stretching vibration of water that interacts weakly with hydrophobic regions of the protein at the interface.^{70,71}

HD-VSFG studies on the monolayers of charged surfactants⁴² and charged lipids⁴⁴ formed at the air/aqueous solution interfaces showed that the orientation of interfacial water changes depending on the charge of the monolayer headgroups. H-up and H-down orientations of water molecules are induced at negatively charged and positively charged interfaces, respectively. The negative OH band observed at pH 5 and the positive OH band observed at pH 9 are well consistent with this scenario: the observed flip-flop of water is induced by the change in the sign of the net charge of the protein. The isoelectric point refers to the pH at which the net charge of the protein is zero. Therefore, it is expected that water orientation at the interface becomes minimum at the isoelectric point because no potential variation influences the water dipole at the interface (Fig. 4). Given its isoelectric point at 7.0 in the bulk,⁵⁴ one could have expected a minimum signal appearing around pH 7. In this regard, it is surprising to observe the intensity minimum of the OH stretching band at pH 6 for HbA. In fact, it has been reported for several proteins that the VSFG or SHG of aqueous/mineral interfaces showed an intensity minimum at the bulk isoelectric points of the protein.^{72,73} For example, Kim *et al.* and

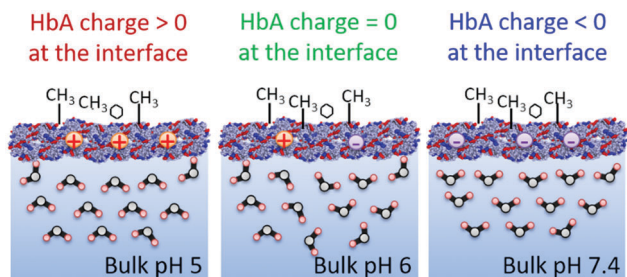


Fig. 4 Schematic representation of the orientation of interfacial water molecules at HbA adsorbed aqueous interface as a function of bulk pH.

Engelhardt *et al.* reported that the OH band intensity measured by conventional VSGF exhibited a minimum for Lz,³⁹ BSA,⁵ and β -lactoglobulin³³ at the corresponding bulk isoelectric point of each protein. Furthermore, the Bakker group reported in their recent HD-VSGF study that α -lactalbumin/water interface exhibited an OH band minimum at the bulk isoelectric point of α -lactalbumin.⁵² This report is particularly important as they measured the $\text{Im} \chi^{(2)}$ spectra which are free from interferences that are inevitable in conventional homodyne detection. Contrary to other VSGF and SHG studies of charged interfaces, in the present study, the minimum of the OH band intensity is observed at pH 6, which is one pH unit lower than the bulk isoelectric point of HbA. This result suggests that the isoelectric point of HbA is shifted to pH ~ 6 when it is adsorbed at the air/water interface (Fig. 4). The validity of this interpretation will be further discussed in the last section.

Orientation of water molecules with various proteins at the air/water interface

In addition to HbA, we measured the $\text{Im} \chi^{(2)}$ spectra of BSA, Mb and Lz at fixed pH 7.4 to compare the orientation of interfacial water molecules with proteins of different charges adsorbed at the air/water interface (Fig. 5). The isoelectric points of these proteins in the bulk are ~ 4.8 for BSA,⁵³ 7.0 for HbA,⁵⁴ 7.4 for Mb,^{55,56}

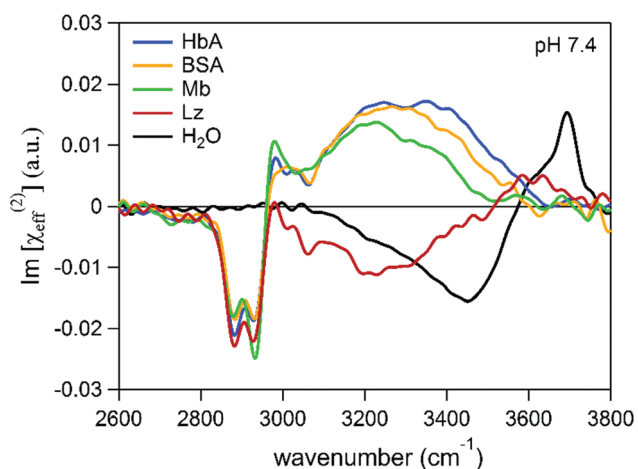


Fig. 5 Imaginary $\chi^{(2)}$ spectra in the CH and OH stretching region of 10 μM HbA, BSA, Mb and Lz in 50 mM phosphate buffer at pH 7.4 at the air/water interface.

and 11.3 for Lz.⁵⁷ At pH 7.4, BSA is negatively charged, Lz is positively charged, HbA and Mb are close to their isoelectric point in the bulk. All the proteins showed high affinity for the air/water interface as evidenced by the intense CH bands of methyl groups at $\sim 2880 \text{ cm}^{-1}$, $\sim 2930 \text{ cm}^{-1}$ and $\sim 2980 \text{ cm}^{-1}$, as well as the complete disappearance of the free OH band at 3700 cm^{-1} . The negative sign of the former two CH bands in the $\text{Im} \chi^{(2)}$ spectrum indicates an average H-up orientation of the methyl groups for the four proteins. A slight difference in the CH stretching bands is observed for Mb: the intensity of the $\sim 2930 \text{ cm}^{-1}$ band is substantially larger than the $\sim 2880 \text{ cm}^{-1}$ band for Mb, whereas the intensities of these two bands are comparable for other proteins. Such a difference in the CH band shape in the VSGF spectra of the self-assembled monolayer has been attributed to different average tilt angles of the methyl groups.⁷⁴ Moreover, Mb is the only protein that does not exhibit the aromatic CH band at $\sim 3060 \text{ cm}^{-1}$, which suggests a somewhat different protein conformation at the interface. For all the proteins, the free OH band disappears, suggesting that the surface is completely covered by adsorbed proteins at 10 μM concentration at pH 7.4. The hydrophobic OH stretching band at $\sim 3600 \text{ cm}^{-1}$ is observed for Lz as in the case of HbA at pH 5.

The H-bonded OH stretching bands of adsorbed proteins in Fig. 5 display opposite signs and different frequency shifts depending on the adsorbed protein. The sign of the OH stretching band indicates H-down water orientation for adsorbed Lz and H-up water orientation for adsorbed Mb, HbA and BSA. The bulk isoelectric points of Lz and BSA are far from the present condition (pH 7.4) and therefore Lz and BSA are expected to be positively and negatively charged, respectively. This is consistent with the charge indicated by the water orientation observed. In contrast, the H-up orientation of water molecules at the Mb interface suggests that the protein is negatively charged at the air/water interface, as observed for HbA, even though the bulk isoelectric point is close to the present pH (7.4 for Mb and 7.0 for HbA). The intensity of the OH stretching band is smaller for Mb, indicating that the net charge of adsorbed Mb is less than that of adsorbed HbA.

For negatively charged proteins, it looks that the H-bonded OH band shows gradual red shifts with the decrease of the integrated band intensity in the order of HbA > BSA > Mb. It might suggest that stronger H-bonding between nearby water molecules and the protein at the air/water interface results in less net water orientation in total. However, the reason of this observation is not clear at the moment because the H-bonding strength between water molecules and a protein may not solely depend on the protein charge but also varies with the protein composition and conformation, which provide different local environments for the surrounding water.

Discussion

Assignment of the OH stretching band intensity minimum

In this section, we discuss the validity of the assignment of the pH value of the minimum OH stretching band intensity to the isoelectric point of the adsorbed protein. At the beginning,

we discuss two other possibilities. First, we consider the possible effect of phosphate buffer on the isoelectric point of HbA. The isoelectric point is the point of zero net charge of a protein under specific salt and buffer conditions, whereas the isoionic point is the point of zero net charge of a protein in pure water.⁷⁵ Thus the isoelectric point may vary depending on the nature and the concentration of the ionic species in solution.⁷⁶ The isoelectric point of HbA measured by zeta potential in our experimental conditions is 7.0 ± 0.1 in phosphate buffer (data not shown). As a control, we also performed the HD-VSFG experiment in pure water. The pH of HbA solution is ~ 7.2 and the isoionic point of HbA is 7.1,^{77–79} implying that bulk HbA is close to neutral in these conditions. The $\text{Im } \chi^{(2)}$ spectrum of HbA in pure water (Fig. S5, ESI†) exhibits a positive OH stretching band indicating H-up water orientation. This suggests that adsorbed HbA is negatively charged at the air/water interface even without phosphate buffer. It confirms that the H-up orientation of water molecules and the shift of the isoelectric point of HbA at the air/water interface are not predominantly due to phosphate buffer but are attributable to the adsorbed HbA.

Second, we discuss the possibility that the “apparent” shift of the isoelectric point of the adsorbed protein arises from the pH change at the air/water interface.^{29,30,80} In general, the pH at the air/water interface can be different from that in the bulk, and recent experimental and theoretical studies indicate that interfacial pH is lower due to the surface affinity of H_3O^+ and bulk preference of OH^- in bulk neat water.^{29–31,81} However, in the case of an aqueous interface covered by proteins, the water molecules which are probed are localized at the protein/water interface. Therefore, the pH shift at the air/water interface is not directly related to the shift of the apparent isoelectric point of the protein at the interface. Moreover, the deviation of surface pH is supposed to induce the same effect on any proteins at the interface, but it is not the case as several proteins exhibit a VSFG intensity minimum around their bulk isoelectric point.^{33,52} Thus, the intrinsic pH shift at the bare air/water interface does not account for the observed shift of the isoelectric point of HbA and Mb at the water surface.

Then, we examine the validity of our interpretation that the VSFG minimum indicates the isoelectric point of a protein at the interface. In this context, we need to note that, at a zwitterionic lipid water interface, a net positive OH band consisting of H-up and H-down orientation of water molecules was observed by HD-VSFG despite the net neutral charge of the lipid.^{70,82} This behavior was explained by the different charge density of positively charged choline and negatively charged phosphate moieties and by the higher solvent accessibility of negatively charged groups in the lipid structure.⁷⁰ Following this, one might think that the minimum intensity of the OH band may not correspond to the isoelectric point of a protein at the interface. However, the isoelectric point, which is determined as the point of zero global charge in electrophoresis, does not correspond only to charge neutralization but also additionally depends on dipole contributions. Indeed, liposomes composed of zwitterionic lipids show non-zero zeta potentials in bulk electrophoresis, which are attributed to the dipole contribution.⁸³ Thus, the observation

of the net positive OH band at the zwitterionic lipid interface does not conflict with the empirical rule that the OH band in the VSFG spectrum is minimum at the isoelectric point of the protein. Moreover, the Bakker group reported that the OH band intensity in the $\text{Im } \chi^{(2)}$ spectrum becomes minimum at the bulk isoelectric point of α -lactalbumin.⁵² In proteins, positive charges are essentially carried by the amino and guanidino moieties of Lys and Arg residues, whereas negative charges are carried by the carboxylate moieties of Glu and Asp residues. Because these charged moieties are common to all proteins,⁸⁴ it is very unlikely that the minimum of the OH band intensity is observed at the isoelectric point for some proteins but not for the others. Rather, it is much more reasonable to consider that the isoelectric point of a protein is held in some proteins but is shifted in others, possibly due to the different extents of protein reorganization at the interface. Furthermore, the charge distributions of the side chains calculated by quantum chemical calculations are comparable for positively charged and negatively charged residues (Fig. S6, ESI†). This suggests that if the exposure to the solvent is the same, the negative residues cannot induce a much larger orientation of the water dipole than the positive residues, contrary to the case of zwitterionic lipid interfaces. By contrast, it is readily expected that the charge distribution of the residue depends on the protein structure that determines the local environment and hydration state of each residue and hence that the structural change of the protein induces a shift of the pK_a of the residues. Thus, the sole charge density of each isolated moiety cannot account for the present shift of the isoelectric point of HbA and Mb at the air/water interface. Based on these considerations, we can conclude that the observed OH band minimum of HbA at pH 6 is attributable to the shift of the isoelectric point of the protein adsorbed at the air/water interface.

Possible mechanisms for the shift of the isoelectric point of the proteins at the air/water interface

The average orientation of water molecules probed by HD-VSFG in the present study can be interpreted as the effect of the electrochemical potential of the protein adsorbed at the air/water interface on the surrounding water molecules.^{85,86} The H-up orientation of water molecules at pH 7.4, close to the isoelectric point of HbA and Mb in the bulk, indicates that both proteins have a negative potential when adsorbed at the air/water interface. Moreover, the minimum intensity of the OH band in the $\text{Im } \chi^{(2)}$ spectrum at pH 6 suggests that the isoelectric point of HbA decreases by one pH unit when adsorbed at the air/water interface. This result is notably different from previous VSFG and SHG studies that reported a similar isoelectric point in the bulk and at the air/water interface for Lz,³⁹ BSA,⁵ α -lactalbumin,⁵² and β -lactoglobulin.³³ It highlights the difference in protein structural reorganization at the air/water interface.

HbA is composed of 78 acid residues (Glu, Asp) and 74 basic residues (Lys, Arg) located in both α -chains and β -chains of the tetramer (Fig. 2b). The negative charge of adsorbed HbA at pH 7.4 implies that a greater number of Glu and Asp groups are deprotonated and/or a fewer number of Lys and Arg groups are protonated at the interface. It is widely known that the

structure of proteins changes when they are adsorbed at the interface (surface denaturation). The shift of the protein isoelectric point at the interface can be induced by a change of the tertiary or secondary structure of the protein during adsorption which leads to a different exposure of charged residues and hence a different solvation state. The substantial change of the adsorbed protein structure is expected to alter the pK_a of the charged residues by several possible mechanisms: the exposure and solvation of charged residues that were buried in the protein structure, the disruption or formation of new attractive and repulsive charge–charge interactions with neighboring groups, and the disruption or formation of H-bonds in charge–dipole interactions.⁸⁴ A large number of studies have reported the structural change of proteins at the air/water interface.^{10,50,69,87,88} For example, Holt *et al.* reported that Mb forms a monolayer at the air/water interface at a concentration of 6 μM and a partial multilayer above 30 μM .⁸⁸ They found that the thickness of the first layer, either in a monolayer or in a partially filled multilayer, is smaller than the size of the native protein. Hence, it is evident that the adsorbed protein structure is altered, and this was attributed to a partial loss of tertiary structure. Therefore, the structural change of the adsorbed proteins is likely to be responsible for the alteration of HbA charge at the air/water interface. The magnitude of this effect would depend on the protein because the degree of structural change at the air/water interface should be protein-dependent. Thus, this mechanism can explain why other proteins adsorbed at the air/water interface and at mineral/water interfaces showed a similar isoelectric point to the bulk. In fact, the observation of the negative CH bands of the protein in the present study indicates that more aliphatic residues become exposed to the air, being in harmony with structural modifications of the protein occurring during adsorption at the air/water interface.¹⁰

A preferential orientation of the proteins, which makes some domains specifically exposed to the air, may also alter the protein charge at the interface. This effect may be important for Mb which has a more asymmetric charge distribution showing clusters of charged residues at its surface (Fig. S4, ESI[†]). In this case, it is readily anticipated that significant changes in the hydration state of the charged residues occur with adsorption at the air/water interface, which can cause the shift of pK_a of the residues and hence a change of the isoelectric point of the protein.

HbA is a tetrameric protein in which α -chains and β -chains have different isoelectric points: 7.5–7.8 for α -chains and 6.1–6.7 for β -chains.⁵⁵ If the adsorbed protein is oriented in such a way that one subunit becomes less exposed to the solvent than the other, then the overall isoelectric point of the tetramer would be altered. Moreover, if the tetramer dissociates and one of the two subunits is preferentially adsorbed at the air/water interface, as observed for insulin,⁸⁹ the charge of the protein probed at the interface would also change. Nevertheless, the surface pressure analysis of the methemoglobin monolayer at the air/water interface showed that the protein retains its native quaternary structure at the interface, which is an equilibrium between dimers ($\alpha\beta$) and tetramers ($\alpha_2\beta_2$) depending on the conditions.⁹⁰ Thus, HbA dissociation is not considered as the main factor for the change

of HbA charge at the air/water interface, and the preferential orientation may play a role. We think that the change of the charge of hemoglobin, which is a tetrameric protein, and myoglobin, which is a monomeric protein, is induced by similar mechanisms at the air/water interface.

Gao *et al.* measured the isoelectric point of bovine HbA immobilized in nanochannels and observed a decrease of the isoelectric point to 6.6 due to confinement.⁹¹ It shows that the change of the environment alters the charge state of HbA to a large extent. Interestingly, two very different stresses, *i.e.* exposure to the air/water interface and confinement in nanochannels, result in a decrease of the protein isoelectric point. On the other hand, others proteins such as BSA,^{5,34} Lz³⁹ and α -lactalbumin⁵² were reported to keep the same isoelectric point at the air/water interface and in the bulk. This difference suggests that some proteins are more sensitive than others to the environment and more largely change their structure, causing a significant shift of their isoelectric points.

It would be very interesting to study the effect of pH for other proteins, and to clarify whether a change of the isoelectric point is specific to hemoglobin and myoglobin or if it is common to a broader diversity of proteins. A change of the protein charge could have major impacts on many biological processes in which finely tuned electrostatic interactions are involved, such as protein–protein interactions or interaction relevant to molecular recognitions. The present study evidences the need to reconsider the effect of protein charges at various interfaces, *e.g.* biocompatible materials or biosensors, and to deepen our understanding on the structural change of proteins at interfaces at the molecular and residue levels.

Conclusion

In summary, we measured the $\text{Im } \chi^{(2)}$ spectra of HbA, Mb, BSA and Lz solutions at the air/water interface in the CH and OH stretching regions by using HD-VSFG spectroscopy, and we deduced the net charge of HbA adsorbed at the air/water interface by detecting the orientational flip-flop of water molecules at the interface. Direct measurements of the sign of $\text{Im } \chi^{(2)}$ as a function of bulk pH indicate that the isoelectric point of HbA is shifted from pH 7.0 in the bulk to pH ~ 6 at the air/water interface. A similar change of the isoelectric point was also suggested for myoglobin adsorbed at the air/water interface. The shift of the isoelectric point at the interface is likely due to the change of the protein conformation and local hydration state at the interface. A preferential orientation of the adsorbed protein may also contribute to this effect. Contrary to previous studies on other model proteins, a significant change of the protein charge is observed at the interface by HD-VSFG, highlighting the different extents of structural reorganization of proteins at the air/water interface. This requests reconsideration of the effect of interfaces on the protein charge.

HD-VSFG is a powerful experimental method to study liquid interfaces at the molecular level. The present study showed that HD-VSFG is also a promising technique to investigate protein

adsorption as well as a relevant interfacial water structure with high specificity and sensitivity. The evidence of a change of HbA and Mb charge at the air/water interface opens the way to more systematic studies on the protein charge at various interfaces. Indeed, a change of protein charge could impact ligand binding or protein–protein interactions in which electrostatic forces are involved. Thus, this effect may be of major relevance for the interactions between materials and complex biological media, which are essential, for example, in material biocompatibility or sensor biofouling.

Acknowledgements

This work was partly supported by JSPS KAKENHI Grant number JP25104005. S. D. gratefully acknowledges the Japan Society for the Promotion of Science for funding through the JSPS Summer Program. K. I. and R. K. acknowledge the Special Postdoctoral Researcher (SPR) Program of RIKEN.

References

- 1 M. N. Gupta, M. Kaloti, M. Kapoor and K. Solanki, *Artif. Cells, Blood Substitutes, Biotechnol.*, 2011, **39**, 98–109.
- 2 T. Jesionowski, J. Zdarta and B. Krajewska, *Adsorption*, 2014, **20**, 801–821.
- 3 S. K. Vashist, C. K. Dixit, B. D. MacCraith and R. O’Kennedy, *Analyst*, 2011, **136**, 4431.
- 4 M. A. Bos and T. van Vliet, *Adv. Colloid Interface Sci.*, 2001, **91**, 437–471.
- 5 K. Engelhardt, A. Rumpel, J. Walter, U. Kulozik, B. Braunschweig and W. Peukert, *Langmuir*, 2012, **28**, 7780–7787.
- 6 P. A. Wierenga and H. Gruppen, *Curr. Opin. Colloid Interface Sci.*, 2010, **15**, 365–373.
- 7 N. Wisniewski and M. Reichert, *Colloids Surf., B*, 2000, **18**, 197–219.
- 8 S. Chen, L. Li, C. Zhao and J. Zheng, *Polymer*, 2010, **51**, 5283–5293.
- 9 K. Yu, B. F. L. Lai, J. H. Foley, M. J. Krisinger, E. M. Conway and J. N. Kizhakkedathu, *ACS Nano*, 2014, **8**, 7687–7703.
- 10 D. L. Leiske, I. C. Shieh and M. L. Tse, *Langmuir*, 2016, **32**, 9930–9937.
- 11 I. Banerjee, R. C. Pangule and R. S. Kane, *Adv. Mater.*, 2011, **23**, 690–718.
- 12 E. Bulard, M.-P. Fontaine-Aupart, H. Dubost, W. Zheng, M.-N. Bellon-Fontaine, J.-M. Herry and B. Bourguignon, *Langmuir*, 2012, **28**, 17001–17010.
- 13 E. Gogolides, K. Ellinas and A. Tserepi, *Microelectron. Eng.*, 2015, **132**, 135–155.
- 14 K. K. Chittur, *Mater. Eng.*, 1998, **19**, 357–369.
- 15 M. D. Lad, F. Birembaut, J. M. Matthew, R. a Frazier and R. J. Green, *Phys. Chem. Chem. Phys.*, 2006, **8**, 2179–2186.
- 16 J. Buijs and V. Hlady, *J. Colloid Interface Sci.*, 1997, **190**, 171–181.
- 17 E. V. Kudryashova, M. B. J. Meinders, a. J. W. G. Visser, A. van Hoek and H. H. J. de Jongh, *Eur. Biophys. J.*, 2003, **32**, 553–562.
- 18 P. Sen, S. Yamaguchi and T. Tahara, *J. Phys. Chem. B*, 2008, **112**, 13473–13475.
- 19 W. Norde and J. P. Favier, *Colloids Surf.*, 1992, **64**, 87–93.
- 20 H. Elwing, *Biomaterials*, 1998, **19**, 397–406.
- 21 C. Postel, O. Abillon and B. Desbat, *J. Colloid Interface Sci.*, 2003, **266**, 74–81.
- 22 J. R. Lu, X. Zhao and M. Yaseen, *Curr. Opin. Colloid Interface Sci.*, 2007, **12**, 9–16.
- 23 C. Czeslik, C. Royer, T. Hazlett and W. Mantulin, *Biophys. J.*, 2003, **84**, 2533–2541.
- 24 G. P. Drobny, J. R. Long, W. J. Shaw, M. Cotten and P. S. Stayton, *Encycl. Magn. Reson.*, 2007, 1–11.
- 25 S. Devineau, J. M. Zanotti, C. Loupiac, L. Zargarian, F. Neiers, S. Pin and J. P. Renault, *Langmuir*, 2013, **29**, 13465–13472.
- 26 R. A. Latour and L. L. Hench, *Biomaterials*, 2002, **23**, 4633–4648.
- 27 Q. Wei, T. Becherer, S. Angioletti-Uberti, J. Dzubiella, C. Wischke, A. T. Neffe, A. Lendlein, M. Ballauff and R. Haag, *Angew. Chem., Int. Ed.*, 2014, **53**, 8004–8031.
- 28 J. Kim and P. S. Cremer, *ChemPhysChem*, 2001, **2**, 543–546.
- 29 V. Buch, A. Milet, R. Vacha, P. Jungwirth and J. P. Devlin, *Proc. Natl. Acad. Sci. U. S. A.*, 2007, **104**, 2–7.
- 30 J. S. Hub, M. G. Wolf, C. Coleman, P. J. van Maaren, G. Groenhof and D. van der Spoel, *Chem. Sci.*, 2014, **5**, 1745–1749.
- 31 S. Yamaguchi, A. Kundu, P. Sen and T. Tahara, *J. Chem. Phys.*, 2012, **137**, 1–5.
- 32 S. Sen, S. Yamaguchi and T. Tahara, *Angew. Chem., Int. Ed.*, 2009, **48**, 6439–6442.
- 33 K. Engelhardt, M. Lexis, G. Gochev, C. Konnerth, R. Miller, N. Willenbacher, W. Peukert and B. Braunschweig, *Langmuir*, 2013, **29**, 11646–11655.
- 34 K. S. Birdi and A. Nikolov, *J. Phys. Chem.*, 1979, **83**, 365–367.
- 35 Q. Du, R. Superfine, E. Freysz and Y. Shen, *Phys. Rev. Lett.*, 1993, **70**, 2313–2316.
- 36 J. Wang, S. M. Buck and Z. Chen, *J. Phys. Chem. B*, 2002, **106**, 11666–11672.
- 37 Y. R. Shen and V. Ostroverkhov, *Chem. Rev.*, 2006, **106**, 1140–1154.
- 38 S. Roke, *ChemPhysChem*, 2009, **10**, 1380–1388.
- 39 G. Kim, M. Gurau, J. Kim and P. S. Cremer, *Langmuir*, 2002, **18**, 2807–2811.
- 40 J. Wang, S. M. Buck and Z. Chen, *Analyst*, 2003, **128**, 773.
- 41 X. Chen, S. C. Flores, S. M. Lim, Y. Zhang, T. Yang, J. Kherb and P. S. Cremer, *Langmuir*, 2010, **26**, 16447–16454.
- 42 S. Nihonyanagi, S. Yamaguchi and T. Tahara, *J. Chem. Phys.*, 2009, **130**, 204704.
- 43 N. Ji, V. Ostroverkhov, C. S. Tian and Y. R. Shen, *Phys. Rev. Lett.*, 2008, **100**, 1–4.
- 44 J. A. Mondal, S. Nihonyanagi, S. Yamaguchi and T. Tahara, *J. Am. Chem. Soc.*, 2010, **132**, 10656–10657.
- 45 S. Nihonyanagi, J. A. Mondal, S. Yamaguchi and T. Tahara, *Annu. Rev. Phys. Chem.*, 2013, **64**, 579–603.
- 46 P. C. Singh, K. Inoue, S. Nihonyanagi, S. Yamaguchi and T. Tahara, *Angew. Chem., Int. Ed.*, 2016, **55**, 10621–10625.
- 47 A. Adhikari, S. Re, W. Nishima, M. Ahmed, S. Nihonyanagi, J. B. Klauda, Y. Sugita and T. Tahara, *J. Phys. Chem. C*, 2016, **120**, 23692–23697.

- 48 S. Nihonyanagi, S. Yamaguchi and T. Tahara, *J. Am. Chem. Soc.*, 2014, **136**, 6155–6158.
- 49 K. Inoue, S. Nihonyanagi, P. C. Singh, S. Yamaguchi and T. Tahara, *J. Chem. Phys.*, 2015, **142**, 212431.
- 50 M. Okuno and T. Ishibashi, *J. Phys. Chem. C*, 2015, **119**, 9947–9954.
- 51 K. Meister, S. Lotze, L. L. C. Olijve, A. L. DeVries, J. G. Duman, I. K. Voets and H. J. Bakker, *J. Phys. Chem. Lett.*, 2015, **6**, 1162–1167.
- 52 S. Strazdaite, K. Meister and H. J. Bakker, *Phys. Chem. Chem. Phys.*, 2016, **18**, 7414–7418.
- 53 E. G. Young, *Comprehensive Biochemistry*, 1963.
- 54 J. M. Hempe and R. D. Craver, *Electrophoresis*, 2000, **21**, 743–748.
- 55 E. Antonini and M. Brunori, *Hemoglobin and Myoglobin in their interactions with ligands. Frontiers of Biology*, North Holland Publishing Company, 1971.
- 56 S. Pin, B. Hickel and B. Alpert, *J. Am. Chem. Soc.*, 1997, **7863**, 10810–10814.
- 57 L. R. Wetter and H. F. Deutsch, *J. Biol. Chem.*, 1951, **192**, 237–242.
- 58 M. F. Perutz, *J. Cryst. Growth*, 1968, **2**, 54–56.
- 59 S. El Antri, O. Sire and B. Alpert, *Eur. J. Biochem.*, 1990, **191**, 163–168.
- 60 R. Banerjee, Y. Alpert, F. Leterrier and R. J. Williams, *Biochemistry*, 1969, **8**, 2862–2867.
- 61 S. Nihonyanagi, R. Kusaka, K. Inoue, A. Adhikari, S. Yamaguchi and T. Tahara, *J. Chem. Phys.*, 2015, **143**, 124707.
- 62 S. A. Hall, K. C. Jena, T. G. Trudeau and D. K. Hore, *J. Phys. Chem. C*, 2011, **115**, 11216–11225.
- 63 S. Nihonyanagi, A. Eftekhari-Bafrooei and E. Borguet, *J. Chem. Phys.*, 2011, **134**, 084701.
- 64 S. A. Hall, A. D. Hickey and D. K. Hore, *J. Phys. Chem. C*, 2010, **114**, 9748–9757.
- 65 K. Engelhardt, U. Weichsel, E. Kraft, D. Segets, W. Peukert and B. Braunschweig, *J. Phys. Chem. B*, 2014, **118**, 4098–4105.
- 66 T. Zoungrana, G. Findenegg and W. Norde, *J. Colloid Interface Sci.*, 1997, **190**, 437–448.
- 67 W. Norde, *Colloids Surf., B*, 2008, **61**, 1–9.
- 68 S. Devineau, M. Anyfantakis, L. Marichal, L. Kiger, M. Morel, S. Rudiuk and D. Baigl, *J. Am. Chem. Soc.*, 2016, **138**, 11623–11632.
- 69 J. R. Lu, T. J. Su and B. J. Howlin, *J. Phys. Chem. B*, 1999, **103**, 5903–5909.
- 70 J. A. Mondal, S. Nihonyanagi, S. Yamaguchi and T. Tahara, *J. Am. Chem. Soc.*, 2012, **134**, 7842–7850.
- 71 G. Ma, X. Chen and H. C. Allen, *J. Am. Chem. Soc.*, 2007, **129**, 14053–14057.
- 72 A. G. Stack, S. R. Higgins and C. M. Eggleston, *Geochim. Cosmochim. Acta*, 2001, **65**, 3055–3063.
- 73 S. Dewan, M. S. Yeganeh and E. Borguet, *J. Phys. Chem. Lett.*, 2013, **4**, 1977–1982.
- 74 B. Bourguignon, W. Zheng, S. Carrez, A. Ouvrard, F. Fournier and H. Dubost, *Phys. Rev. B: Condens. Matter Mater. Phys.*, 2009, **79**, 125433.
- 75 W. P. Bryan, *Biochem. Educ.*, 1978, **6**, 14–15.
- 76 S. Salgin, U. Salgin and S. Bahadir, *Int. J. Electrochem. Sci.*, 2012, **7**, 12404–12414.
- 77 I. H. Schneiberg, R. S. Harris and J. L. Spitzer, *Proc. Natl. Acad. Sci. U. S. A.*, 1954, **40**, 777–783.
- 78 C. Tanford and Y. Nozaki, *J. Biol. Chem.*, 1966, **241**, 2832–2839.
- 79 V. Le Tilly, *Etude des interactions intraprotéiques dans la metmyoglobine de cheval*, PhD thesis, Université Paris 7, 1991.
- 80 A. Kundu, S. Yamaguchi and T. Tahara, *J. Phys. Chem. Lett.*, 2014, **5**, 762–766.
- 81 Y.-L. S. Tse, C. Chen, G. E. Lindberg, R. Kumar and G. A. Voth, *J. Am. Chem. Soc.*, 2015, **137**, 12610–12616.
- 82 S. Re, W. Nishima, T. Tahara and Y. Sugita, *J. Phys. Chem. Lett.*, 2014, **5**, 4343–4348.
- 83 K. Makino, T. Yamada, M. Kimura, T. Oka, H. Ohshima and T. Kondo, *Biophys. Chem.*, 1991, **41**, 175–183.
- 84 C. N. Pace, G. R. Grimsley and J. M. Scholtz, *J. Biol. Chem.*, 2009, **284**, 13285–13289.
- 85 S. N. Timasheff, *Biochemistry*, 2002, **41**, 13473–13482.
- 86 S. N. Timasheff, *Proc. Natl. Acad. Sci. U. S. A.*, 2002, **99**, 9721–9726.
- 87 J. R. Lu, T. J. Su and R. K. Thomas, *J. Colloid Interface Sci.*, 1999, **213**, 426–437.
- 88 S. A. Holt, D. J. McGillivray, S. Poon and J. W. White, *J. Phys. Chem. B*, 2000, **104**, 7431–7438.
- 89 S. Mauri, T. Weidner and H. Arnolds, *Phys. Chem. Chem. Phys.*, 2014, **16**, 26722–26724.
- 90 J. Kubicki, H. D. Ohlenbusch, E. Schroeder and A. Wollmer, *Biochemistry*, 1976, **15**, 5698–5702.
- 91 H.-L. Gao, C.-Y. Li, F.-X. Ma, K. Wang, J.-J. Xu, H.-Y. Chen and X.-H. Xia, *Phys. Chem. Chem. Phys.*, 2012, **14**, 9460.